*Article*

# Physicochemical and Anti-UVB-Induced Skin Inflammatory Properties of *Lacticaseibacillus paracasei* Subsp. *paracasei* SS-01 Strain Exopolysaccharide

Yanfeng Su [1,2,†], Yongtao Zhang [1,†], Hao Fu [1], Feifei Yao [3], Pingping Liu [1], Qiuting Mo [1], Dongdong Wang [1,2], Dan Zhao [1,2], Changtao Wang [1,2] and Meng Li [1,2,*]

1   Key Laboratory of Plant Resources Research and Development, College of Chemistry and Materials Engineering, Beijing Technology and Business University, Beijing 100048, China; 20111006@btbu.edu.cn (Y.S.); 2030402098@st.btbu.edu.cn (Y.Z.); 1930101019@st.btbu.edu.cn (H.F.); liupingping@ynbyjk.com (P.L.); 2130041028@st.btbu.edu.cn (Q.M.); wdd@btbu.edu.cn (D.W.); zhao_dan@btbu.edu.cn (D.Z.); wangct@th.btbu.edu.cn (C.W.)
2   Institute of Cosmetic Regulatory Science, Beijing Technology and Business University, Beijing 100048, China
3   Public of China Changchun Institute of Applied Chemistry, Chinese Academy of Sciences, Changchun 130022, China; ffyao@ciac.ac.cn
*   Correspondence: limeng@btbu.edu.cn; Tel.: +86-134-2601-5179
†   These authors contributed equally to this work.

**Abstract:** The exopolysaccharide secreted by *Lacticaseibacillus paracasei* subsp. *paracasei* SS-01 strain (LP-EPS) is isolated and purified from yogurt. It is a polysaccharide with a branched and multi-stranded structure, which exists in a smooth rod-like or cloud-like state, and possesses a good thermal stability and a molecular weight of 49.68 kDa ($\pm$4.436%). LP-EPS shows a high antioxidant capacity, anti-inflammatory and anti-sensitizing activity during in vitro experimental studies, with half clearance ($IC_{50}$) rates of 0.449, 1.314, and 2.369 mg/mL for the ABTS, DPPH, and OH radicals, respectively, and a half inhibition rate ($IC_{50}$) of hyaluronidase of 1.53 mg/mL. A cell-based assay, enzyme-linked immunosorbent assay (ELISA), and quantitative real-time fluorescence PCR (qRT-PCR) show that LP-EPS effectively treats or ameliorates the skin inflammatory responses triggered by UVB irradiation, as evidenced by a highly significant decrease in the secretion of inflammatory factors by human skin keratinocytes (HaCaT), and a highly significant downregulation of the mRNA expression of MAPK/AP-1 pathway cytokines.

**Keywords:** *Lacticaseibacillus paracasei* subsp. *paracasei*; exopolysaccharides; physicochemical properties; skin inflammation

## 1. Introduction

Microbial exopolysaccharides (EPS) are a class of extracellular sugar metabolites/polymers secreted by microbes [1]. The biological activity and physicochemical properties of EPS are reported to depend on their molecular weight (MW), monosaccharide composition, and structural conformation [2]. There are huge differences in the MW, polysaccharide/monosaccharide composition, connection form, structure, and spatial conformation between the constituent units of EPS [3], resulting in different application values across various fields. Microbial EPS are widely studied and applied in the fields of food, medicine, beauty, and daily chemicals, due to their various physicochemical and functional properties [4,5], with particular research and application of EPS produced by lactic acid bacteria (LAB). These are mostly heteropolysaccharides [6] composed of multiple sugar units, such as pentose, hexose, *N*-acetylated monosaccharides, and uronic acids. LAB EPS can be multi-branched or non-branched, giving them a high thickening ability at low concentrations [7], and a large number of studies show that LAB EPS have good anti-inflammatory, antioxidant, anti-tumor, immune regulation, and anti-aging effects [8–10].

We isolated and purified a strain of *Lacticaseibacillus paracasei* subsp. *paracasei* SS-01 strain from yogurt, one of the most representative strains of LAB [11]. According to the literature, *L. paracasei* subsp. *paracasei* effects the regulating of intestinal and skin inflammation, and its primary functional substance is exopolysaccharides [12–14]. *L. paracasei* subsp. *paracasei* 34-1 is a heteropolysaccharide composed of D-galactose, 2-acetamido-2-deoxy-D-galactose, and sn-glycerol 3-phosphate in a molar ratio of 3:1:1 [15], while *L. paracasei* subsp. *paracasei* DG is a branched-chain heteropolysaccharide, composed of l-rhamnose, D-galactose, and *N*-acetyl-D-galactosamine in a molar ratio of 4:1:1 [16]. It is seen that the EPS of different strains of *L. paracasei* subsp. *paracasei* also have great differences. To investigate the physicochemical and anti-UVB-induced skin inflammatory properties of *L. paracasei* subsp. *paracasei* SS-01 strain extracellular polysaccharides (LP-EPS), its physicochemical properties were analyzed using Fourier transform infrared spectrometry (FT-IR), gel permeation chromatography (GPC), scanning electron microscopy (SEM), atomic force microscopy (AFM), and thermogravimetric analysis (TGA). The antioxidant capacity, anti-inflammatory, and antiallergic activities of LP-EPS were preclinically investigated using a free radical scavenging assay and a hyaluronidase inhibition assay in vitro. To further explore and verify the anti-UVB-induced skin inflammation activity of LP-EPS, we conducted a cell-based assay, ELISA, and qRT-PCR through the established UVB-HaCaT cell model, to evaluate the oxidative stress and inflammatory response of human skin keratinocytes (HaCaT) induced by LP-EPS.

## 2. Materials and Methods

### 2.1. Materials

HaCaT were purchased from National Infrastructure of Cell Line Resource, Beijing, China; *L. paracasei* subsp. *paracasei* SS-01 strain was isolated from yogurt; FM medium, fetal bovine serum, 0.25% trypsin (containing EDTA), and penicillin-streptomycin were purchased from Thermo Fisher Scientific (China) Co., Ltd., Shanghai, China; hydrogen peroxide, salicylic acid, ferrous sulfate, aspirin, hypodexamethasone, and 2,2-diphenyl-1-picrylhydrazyl were purchased from Sinopharm Chemical Reagent Co., Ltd., Beijing, China; Cell Counting Kit-8, First Strand cDNA Synthesis Kit, and Fast Super EvaGreen® qPCR Master Mix were purchased from Biorigin (Beijing, China) Inc.

### 2.2. Culture of L. paracasei Subsp. paracasei SS-01 Strain and Extraction of EPS

In our previous study, *L. paracasei* subsp. *paracasei* SS-01 strain isolated from yogurt was identified by MegaBio, and the reported nucleotide sequence was deposited in GenBank, ID: MW433888.

*L. paracasei* subsp. *paracasei* SS-01 strain was inoculated in 1 L of MRS broth with 5% (*v/v*) culture, and incubated for 48 h at 37 °C. The pH was monitored during fermentation in the range of 3.8−5.0. After the culture was heated to 115 °C for 15 min, cells were removed by centrifugation at 5000 rpm for 10 min at 4 °C.

LP-EPS was extracted according to the ethanol precipitation methods of Liu et al. [17], 80% (*w/v*) ethanol was then added to the cell-free supernatant and it was kept at 4 °C overnight. After alcohol precipitation, the sample was reconstituted with water to its original volume, and papain was added at a volume ratio of 2%. After enzymatic hydrolysis at room temperature for 4 h, it was boiled at 100 °C for 10 min to inactivate the enzymes. Next, alcohol precipitation was conducted again and the precipitate was collected. Crude polysaccharides were obtained after freeze drying. The obtained crude EPS were dissolved in ultrapure water and dialyzed (with 10 kDa MW cut-off) for 48 h at 4 °C, before it was finally lyophilized and named "LP-EPS".

LP-EPS at 1.0 mg/mL was scanned in the 200–600 nm range with a UV spectrophotometer. Observations were then made to determine whether the UV spectrum had a nucleic acid absorption peak at 260 nm, and a protein absorption peak at 280 nm.

### 2.3. FT-IR

According to the method of Yang et al. [9], 1 mg of LP-EPS was ground into a fine powder, mixed with 100 mg of KBr (particle size 200 mesh), then pressed into a thin sheet in a mold. FT-IR analysis was conducted with a Vertex 70 FT-IR spectrometer in transmission mode. The wavelength range was set to 400–4000 cm$^{-1}$, with a resolution of 1 cm$^{-1}$.

### 2.4. GPC, SEM, AFM and TGA

The MW of LP-EPS was determined using gel permeation chromatography—eighteen-angle laser light scattering instrument—differential refractive index detector (GPC-LS-RI), following the previously mentioned method [18].

The determination of the morphological characteristics of LP-EPS was performed using a FEI Nova Nano SEM 450 instrument. A total of 5 mg of LP-EPS was immobilized on the SEM stub and coated with a 10 nm layer of gold, then observed at 250–1000× magnification, at an accelerating voltage of 5.0 kV.

To understand the morphological characteristics of LP-EPS, high-resolution imaging analysis was performed using AFM (Agilent, New York, NY, USA). The sample was dissolved in distilled water (10 µg/mL) and filtered (0.45 µm membrane). A total of 20 µL of the solution was dropped on fresh mica, and dried at room temperature for 24 h. A gas phase probe (ScanAsyst-Air, Bruker AFM Probes, Tokyo, Japan) was used for imaging, used in intelligent imaging mode. The operating mode was ScanAsyst, the scanning speed was 1 Hz, and the scanning area was 2.5 × 2.5 µm.

Under temperature-controlled conditions, thermodynamic analysis methods are often used to measure the relationship between the physical or chemical parameters of a sample and temperature. According to the method of Riaz Rajoka et al. [19], the LP-EPS freeze-dried powder was placed in an $Al_2O_3$ crucible, and heated from 25 °C to 800 °C at a rate of 10 °C min$^{-1}$, in order to observe the state of the sample, and the experiment was performed in an air atmosphere, at a flow rate of 100 mL/min.

### 2.5. Antioxidant Ability and Hyaluronidase Inhibition Assay

In an in vitro antioxidant assay, we formulated LP-EPS at 10, 5, 2.5, 1.25, 0.625, and 0.3125 mg/mL, to investigate its free radical scavenging ability. In addition, 0.03125$^{-2}$ mg/mL ascorbic acid (VC) was prepared as a positive control in vitro antioxidant test. The DPPH radical scavenging activity and hydroxyl radical scavenging activity of LP-EPS were evaluated using the methods described by Min et al. [20,21]. The total antioxidant capacity of LP-EPS was measured using a total antioxidant capacity assay kit with the ABTS method (Beyotime Biotechnology, Beijing, China).

As a participant in Type I allergic reactions, hyaluronidase has a strong correlation with inflammation and allergy, so the inhibition of hyaluronidase activity is used as an indicator to evaluate anti-inflammatory and antiallergic effects on the skin. To explore the potential anti-inflammatory and antiallergic effects of LP-EPS, we measured the inhibitory activity of LP-EPS on hyaluronidase by referring to the method of Lei et al. [22]. A total of 100 µL 2.5 mM $CaCl_2$ and 500 µL 600 U/mL hyaluronidase were added to a test tube and treated at 37 °C for 20 min. Then, 500 µL LP-EPS was added, and treated at 37 °C for 20 min. Subsequently, 500 µL sodium hyaluronate (0.5 mg/mL) was added, and treated for 30 min at 37 °C. After standing at room temperature for 5 min, 500 µL acetyl acetone solution and 100 µL 0.4 M NaOH solution were added, boiled for 15 min, and immediately transferred to an ice bath for 5 min. Next, 1 mL Ehrlich reagent was added, and the absorbance was measured at 530 nm at room temperature for 20 min.

### 2.6. HaCaT Culture and Toxicity Assay

According to the previous method [23], HaCaT (1 × 10$^4$ cells/well) was inoculated into 96-well plates and cultured. The viability of cells treated with LP-EPS and 6 J/cm$^2$ of UVB was determined using CCK8. The OD450 value was measured using a microplate reader (Thermo Fisher Scientific, Waltham, MA, USA).

### 2.7. ROS Assay

According to the previously mentioned method [23], the level of reactive oxygen species (ROS) in the cells was determined using an ROS detection kit (Beyotime Biotechnology, China). The DCFH-DA fluorescent probe was incubated for 20 min, the medium was changed, and the fluorescence intensity of ROS in HaCaT cells was observed under a fluorescent inverted microscope (CKX53, Olympus LS, Tokyo, Japan).

### 2.8. Determination of Inflammation Factor Secretion by ELISA

The cultured medium was collected and centrifuged at 4 °C, 5000 rpm for 10 min to take the supernatant to remove cells suspended in the medium. Inflammation-causing factors interleukin-1β (IL-1β), interleukin-6 (IL-6), and tumor necrosis factor-α (TNF-α) were determined by an ELISA kit (Wuhan Huamei Biological Engineering Co., Ltd., Wuhan, China).

### 2.9. qRT-PCR

The total RNA of HaCaT was extracted with Trizol, and reversely transcribed using a y First Strand cDNA Synthesis Kit. The cDNA obtained by further reverse transcription was tested using the Fast Super EvaGreen$^{®}$ qPCR Master Mix and qRT-PCR (QuantStudio 3, Thermoscientific, Shanghai, China). The relevant primer sequences are shown in Table 1.

**Table 1.** Primer sequences.

| Primers | Primer Sequences (5′—>3′) | Gene ID |
|---|---|---|
| GAPDH | F-AATGGGCAGCCGTTAGGAAA<br>R-GCCCAATACGACCAAATCAGAG | 2597 |
| P38 | F-GGGGCTGAGCTTTTGAAGAA<br>R-CAGCAAGTCGACAGCCAGG | 1432 |
| ERK | F-CCGAGTGACGAGCCCAT<br>R-CTCCCTTGCTAGAGCTCACT | 5594 |
| JNK | F-CTGAAGCAGAAGCTCCACCA<br>R-GCCATTGATCACTGCTGCAC | 5599 |
| Jun | F-TGAGTGACCGCGACTTTTCA<br>R-TTTCTCTAAGAGCGCACGCA | 3725 |
| Fos | F-GGGCAAGGTGGAACAGTTATC<br>R-CAGGTTGGCAATCTCGGTCT | 2353 |

### 2.10. Statistical Analysis

Data visualization and analysis were conducted with Graph Prism 9.2 (GraphPad Software Inc.). The experimental data were verified by 3 parallel and 3 repeated experiments, and all data were represented by mean ± standard deviation. Data variance analysis was conducted by one-way ANOVA ("family-wise alpha thresholds and confidence levels" was set to 0.05 (95% confidence interval), and "statistical hypothesis testing" was set to dunnett test).

## 3. Results

### 3.1. UV-Vis and FT-IR Analysis of EPS

The presence of nucleic acid and protein results in obvious absorption peaks at 260 nm and 280 nm, respectively [9]. In Figure 1a, the absorbance of LP-EPS at 200–600 nm shows no peaks at 260 and 280, meaning that the extraction process is successful, and the LP-EPS is relatively pure.
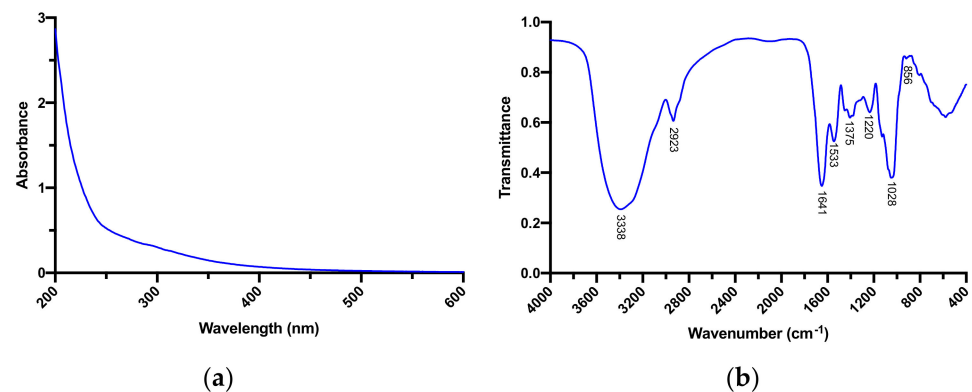
**Figure 1.** Structural characterization of LP-EPS: (**a**) UV absorption peaks of LP-EPS in the range of 200–600; (**b**) IR spectrum of LP-EPS.

The FT-IR spectrum of LP-EPS is shown in Figure 1b. The absorption peak at 3338 cm$^{-1}$ is attributed to the stretching vibration of the hydroxyl group (O-H) [24]. The absorption peak at 2923 cm$^{-1}$ is caused by the stretching vibration of C-H [25]. The absorption peaks at 1641 and 1533 cm$^{-1}$ are attributed to the C=O stretching vibration of LP-EPS [26]. The absorption peak at 1375 cm$^{-1}$ indicates the presence of the carboxyl (COOH) group [27], while the absorption peaks at 1220 cm$^{-1}$ and 1024 cm$^{-1}$ are C-O-C, or C-O stretching vibration peaks, which may represent the presence of sugar or glycoside bonds in the form of pyranose [9]. The main functional groups in LP-EPS, including carboxyl and hydroxyl, determine the physical properties of LP-EPS [21].

*3.2. Physical Properties of EPS*

Dextran standard was used as a reference and marker, and its GPC spectrum is shown in Figure 2a. Both refractive index (RI) and light scattering (LS) detectors show sharp symmetrical peaks that overlap highly. The calculated average MW of the dextran standard is 11.34 kDa ($\pm$1.245%), which is consistent with the MW of the dextran standard, indicating that the system and its operation are normal. The GPC of LP-EPS is shown in Figure 2b and Table 2, and the measured MW of LP-EPS is 49.68 kDa ($\pm$4.436%), which is consistent with previous studies reporting that the Mw of *Lactobacillus* exopolysaccharide is generally in the range of $10^4$–$10^6$ Da [25].
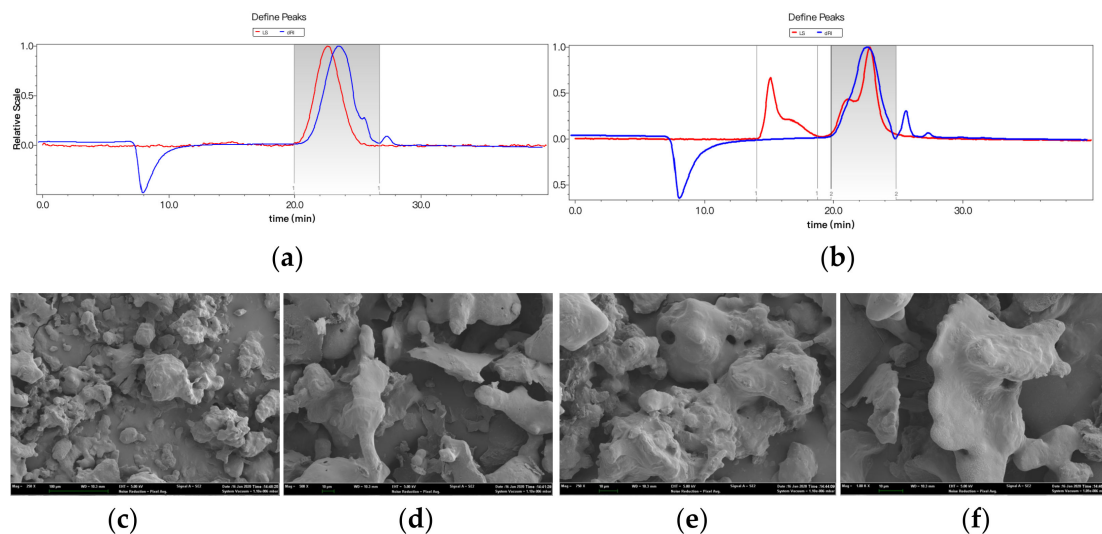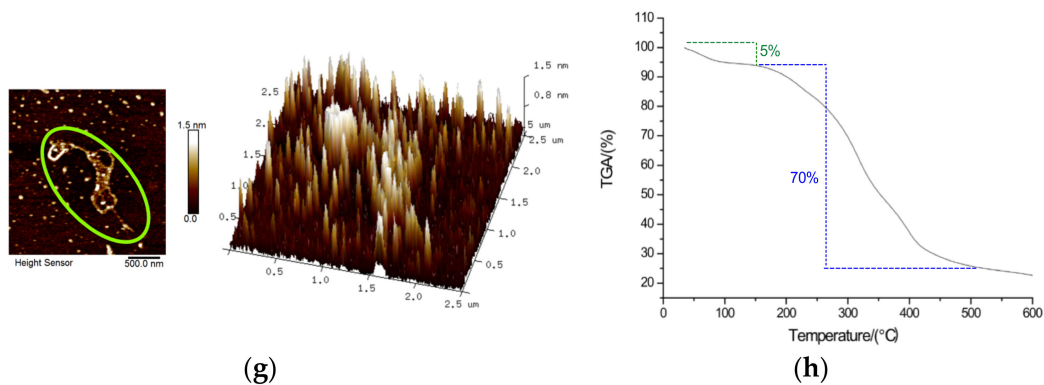


**Figure 2.** *Cont.*

(**g**)

(**h**)

**Figure 2.** Molecular characterization of LP-EPS: (**a**) GPC chromatogram of dextran standard; (**b**) GPC chromatogram of LP-EPS; (**c**) SEM image of LP-EPS (250×); (**d**) SEM image of LP-EPS (500×); (**e**) SEM image of LP-EPS (750×); (**f**) SEM image of LP-EPS (1000×); (**g**) AFM image of LP-EPS; (**h**) TGA analysis of LP-EPS.

**Table 2.** LP-EPS molecular weight determination.

|  | **Dextran Standard** | **LP-EPS** |
|---|---|---|
| Peak name | Peak 1 | Peak 2 |
| Peak limits (min) | 19.952–26.727 | 19.810–24.865 |
| Mw | $1.134 \times 10^4$ ($\pm1.245\%$) | $4.968 \times 10^4$ ($\pm4.436\%$) |
| Mz | $1.900 \times 10^4$ ($\pm2.572\%$) | $5.672 \times 10^4$ ($\pm9.334\%$) |
| Mw/Mn | 2.379 ($\pm13.284\%$) | 1.100 ($\pm6.641\%$) |
| Mz/Mn | 3.988 ($\pm13.473\%$) | 1.256 ($\pm10.562\%$) |

SEM analysis is a powerful tool for observing and analyzing the microscopic morphology of substances. Therefore, we determined the surface morphology of LP-EPS using SEM analysis. Figure 2c–f show images of LP-EPS observed under SEM of 250, 500, 750, and 1000×. The microstructure of LP-EPS presents a smooth and delicate surface in an irregular rod-shaped/cloud-shaped state. The texture is soft and fine, which is in line with the light appearance of the powder. It is speculated that LP-EPS has good water retention capacity and rheological properties.

Along with SEM, AFM is another technique used to characterize matter. Figure 2g shows 2D and 3D AFM images of LP-EPS (10 µg/mL), which reveal intermolecular forces and how the appearance changes from loose points to a network, chain and island structure. There is an obvious height peak in this region, and the width of the peak also increases significantly. This indicates that LP-EPS has a multi-branched chemical structure [28], and it may have more hydroxyl and carboxyl groups, which promote intermolecular interactions.

TGA was used to evaluate the thermal behavior of LP-EPS. As shown in Figure 2h, LP-EPS has two stages of weight loss. In the first stage, from the initial temperature to 150 °C, it loses 5% of its weight due to water evaporation. In the second stage, from 150 °C to 500 °C, there is a 70% weight loss, attributed to thermal decomposition and the breakage of the depolymerized fragments [24]. The final residue of LP-EPS is 25%. These results indicate that LP-EPS has a good thermal stability.

*3.3. In Vitro Antioxidant and Hyaluronidase Inhibitory Capacity of LP-EPS*

An in vitro free radical scavenging experiment was used to verify the antioxidant capacity of LP-EPS quickly and intuitively. The free radical scavenging experiment is shown in Figure 3. The scavenging rates of DPPH, HO·, and ABTS radicals by LP-EPS are proportional to the sample concentrations. High scavenging levels of 73.84%, 88.80%, and 90.46% are achieved when LP-EPS reaches 10 mg/mL for DPPH, hydroxyl radicals, and ABTS, respectively. In addition, the $IC_{50}$ concentrations of LP-EPS on the scavenging rates of DPPH, HO·, and ABTS free radicals are 1.314, 2.369, and 0.449 mg/mL, respectively. On

the other hand, as shown in Figure 3b, the trend of antioxidant capacity of ascorbic acid (VC) is similar to that of LP-EPS, and the scavenging effect achieved at 1 mg/mL is similar to that of LP-EPS at 5 mg/mL. It can be seen that LP-EPS has a strong antioxidant capacity.
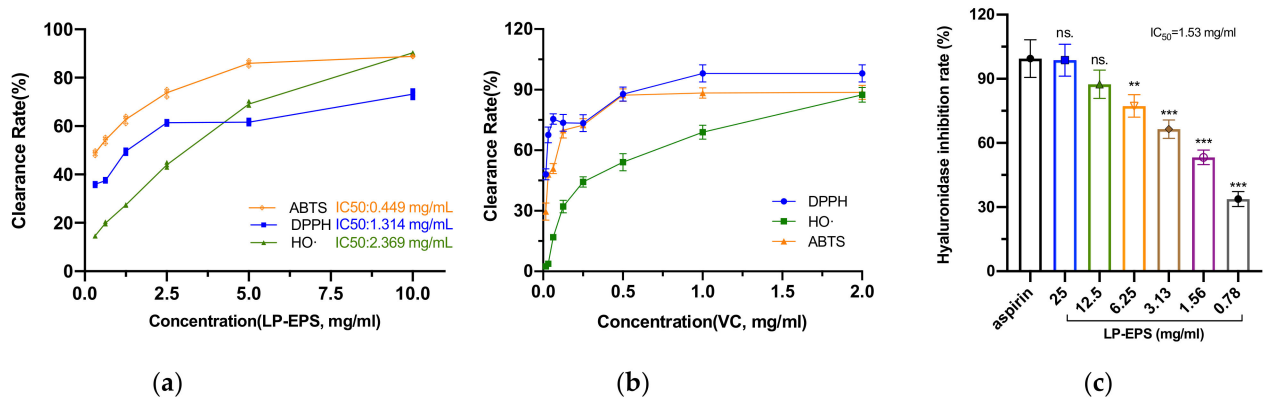


| (a) | (b) | (c) |

**Figure 3.** In vitro biochemical experiments: (**a**) in vitro antioxidant assay of LP-EPS; (**b**) in vitro antioxidant assay of VC; (**c**) hyaluronidase inhibition assay. ns.: $p > 0.05$, **: $p < 0.01$, ***: $p < 0.001$.

Hyaluronidase is a hydrolase that specifically decomposes hyaluronic acid (HA). HA is the main component of the extracellular and intercellular matrix. The decomposition of HA causes cell degranulation and media leakage, leading to rapid skin inflammation and allergic reactions. The inhibitory effects of LP-EPS on hyaluronidase activity are shown in Figure 3c. The inhibitory effects of LP-EPS on hyaluronidase activity are proportional to the sample concentrations. After 12.5 mg/mL, the increase in the inhibition rate tends to become flat, and at 25 mg/mL the inhibitory ability of LP-EPS tends to be about 95%. In addition, the inhibition rates of LP-EPS at 25 and 12.5 mg/mL, and the positive control of aspirin at 5 mg/mL are similar, with no significant difference (ns., $p < 0.05$). According to the data analysis, the half inhibition rate of hyaluronidase is 1.53 mg/mL ($IC_{50}$). This shows that LP-EPS has a certain ability to inhibit the activity of hyaluronidase, giving it potential value in the research and application of anti-inflammatory and anti-allergy treatment.

### 3.4. Cell Viability and ROS Level

To explore the cytotoxicity of LP-EPS, and its protective effects against UVB damage, we treated HaCaT with different concentrations of LP-EPS, in order to detect cell viability. As shown in Figure 3a (left), when the concentration of LP-EPS is less than 5 mg/mL, no cytotoxicity is exhibited. As shown in Figure 3a (right), when HaCaT is treated with 6 J/cm$^2$ UVB, the cell survival rate decreases to about 60%. Fortunately, according to the results of statistical analysis, the cell survival rate significantly improves ($p < 0.001$) in all three concentrations of non-toxic LP-EPS, which is sufficient to prove that LP-EPS protects HaCaT from UVB damage.

ROS include hydroxyl radicals, hydrogen peroxide, etc. An increase in ROS can cause oxidative damage to the intracellular lipids, proteins, and DNA; induce oxidative stress; and lead to inflammation, functional exhaustion, or apoptosis. ROS fluorescence intensity photos of HaCaT treated using a DCFH-DA probe, and taken with an inverted fluorescence microscope, are shown in Figure 4b. The ROS fluorescence intensity of HaCaT, irradiated by UVB, is significantly enhanced, while the light intensity of ROS after LP-EPS treatment improves considerably compared with the UVB model group, and the intensity is similar to that of 50 μg/mL VC.
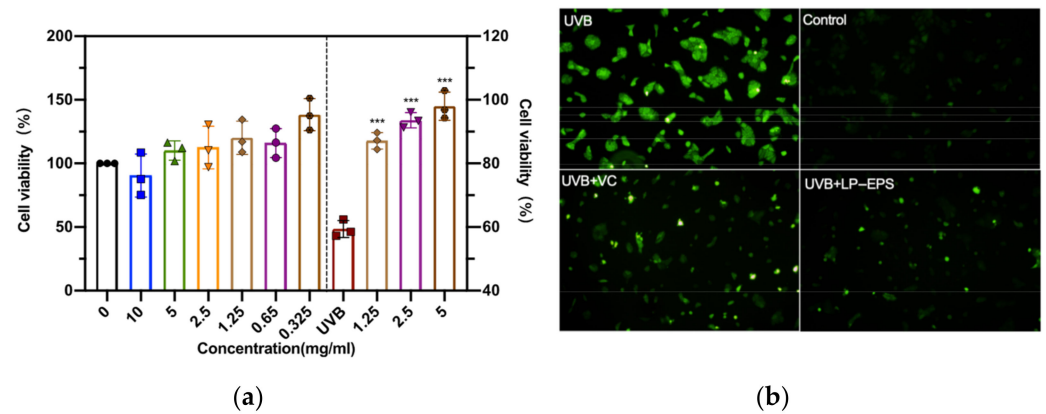
**Figure 4.** Cell experiments: (**a**) HaCaT cell viability: toxicity test (left) and protective effect test (right); (**b**) fluorescence intensity photo of ROS in HaCaT cells. ***: $p < 0.001$.

*3.5. MAPK/AP-1 Pathway and Inflammation Factor*

The activator protein-1 (AP-1) family consists of transcription factors downstream of the MAPK cascade. AP-1 is mainly composed of homologs and heterodimers formed by the FOS and JUN family proteins, and regulated by MAPK, ERK, and JNK [29]. It is reported that AP-1, similar to NF-κ B, contains transcriptional regulatory binding sites for most inflammatory mediators. AP-1 is also independent of the NF-κ B binding promoter during inflammation [30]. Moreover, enhanced AP-1 transcription upregulates the expression of MMP genes (such as MMP-1 and MMP-3), which accelerates the degradation of the intercellular matrix (ECM), and further weakens the skin barrier function [31]. As shown in Figure 5a, in this study the expressions of the transducers (P38 MAPK, ERK, and JNK) and the transcription factors (C-JUN and C-FOS) in the MAPK/AP-1 signaling pathway in HaCaT, with UVB-induced injury, are significantly upregulated ($p < 0.001$), which is a manifestation of inflammation. Compared with the UVB model group, the expression levels of the above factors, measured in HaCaT treated with LP-EPS significantly improve ($p < 0.001$), indicating that LP-EPS has potential anti-inflammatory value.
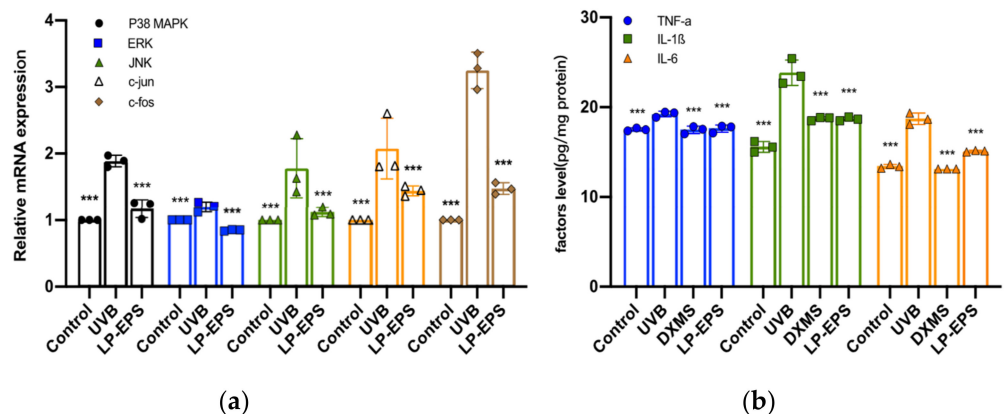


**Figure 5.** Molecular biology level experiments: (**a**) mRNA expression levels of key factors in MAPK signaling pathway; (**b**) levels of key cellular inflammatory factors secreted by HaCaT. ***: $p < 0.001$.

UVB irradiation causes keratinocytes to secrete cytokines such as interleukins (IL-1, IL-3, IL-6, and IL-8) and TNF-α [32]. The main inflammatory factors TNF-α, IL-1β, and IL-6 secreted by HaCaT, measured in this study by ELISA, are shown in Figure 5b. UVB causes the secretion of inflammatory factors of HaCaT to upregulate by varying degrees, especially IL-1β and IL-6. In this experiment, dexamethasone (DXMS) was used as the positive control to observe the effects of LP-EPS. According to the results of statistical analysis, it is shown that the interleukin and TNF-α secreted by HaCaT are significantly

reduced ($p < 0.001$) after LP-EPS treatment, and the effects are close to those of DXMS. It is concluded that LP-EPS effectively regulates the secretion of inflammatory factors in skin epidermal cells.

## 4. Discussion

In this study, LP-EPS was isolated and purified from the metabolites of *L. paracasei* subsp. *paracasei* SS-01 strain. In molecular characterization and characteristic analysis, the results of GPC show that the MW of LP-EPS is low (Mv = 49.68 kDa ($\pm$4.436%)), which is consistent with previous studies that report the MW of *Lactobacillus exopolysaccharide* being within the range of $10^4$–$10^6$ Da [10]. SEM, with a magnification of 250–1000$\times$, shows that LP-EPS has a smooth rod-like or cloud-like state, and the microstructure displayed by AFM shows that LP-EPS has a reasonable intermolecular force, as a kind of polysaccharide with a long-chain branching and multi-strand entangling structure. The intermolecular force is related to -OH and -COOH, and is detected by FT-IR. The TGA of LP-EPS also show a good thermal stability.

LP-EPS is shown to have a significant free radical scavenging ability, and enhanced cellular antioxidant capacity [33]. The results presented in Figure 3a also confirm the antioxidant activity of LP-EPS. In the free radical scavenging assay, 5 mg/mL of LP-EPS presents a higher free radical scavenging efficiency, similar to 1 mg/mL of VC. In the free radical scavenging assay, LP-EPS at 5 mg/mL shows a higher free radical scavenging efficiency, similar to 1 mg/mL VC. Moreover, the concentration of LP-EPS is 1.314, 2.369, and 0.449 mg/mL for 50% scavenging of the DPPH, HO·, and ABTS radicals, respectively, which also indicates that good antioxidant efficiency is achieved at small usage levels. Hyaluronidase is a hydrolase that specifically decomposes hyaluronic acid (HA). HA is the main component of the extracellular and intercellular matrix. The decomposition of HA causes cell degranulation and media leakage, leading to rapid skin inflammation and allergic reactions. According to clinical studies, *L. paracasei* subsp. *paracasei* IJH-SONE68 improves allergic reactions to chronic inflammation [34]. We found strong inhibitory activity of LP-EPS in the hyaluronidase inhibition assay, shown by the fact that 12.5 mg/mL LP-EPS inhibits hyaluronidase at a concentration similar to that of 5 mg/mL aspirin, and the semi-inhibition rate concentration of hyaluronidase is only 1.53 mg/mL, which provides good anti-inflammatory and anti-allergic activity at a lower level of use, which is consistent with the results of Noda et al. [35]. The results of in vitro experiments show both that LP-EPS has great potential, and the value of further research and development in anti-oxidation and anti-inflammatory.

The production of large amounts of ROS induced by UV light can lead to oxidative stress and its cascade reactions. UVB is the main source of daily sunburn and other discomforts, such as erythema [32]. However, the detection of reactive oxygen species in HaCaT cells, as shown in Figure 4b, further confirms that LP-EPS has a strong antioxidant capacity, and effectively removes excess reactive oxygen species in cells. Studies show that human keratinocytes irradiated with UVB over-secrete the inflammatory cytokines IL-1β, IL-6, IL-8, and TNF-α, by activating the NF-κB pathway [36,37]. The functional properties of EPS, in both edible and external use, are widely studied. In the cell experiment part, LP-EPS of under 5 mg shows non-toxic properties, proving the safety of its application. It is also shown to play a highly significant protective role over UVB damaged cells, greatly protecting the skin from UVB sunburn. Our results are also consistent in terms of the inflammatory chemokines and cytokines that are easily induced by UVB. UVB irradiation significantly induces HaCaT to secrete inflammatory cytokines. Fortunately, LP-EPS can effectively reduce such secretion. In addition, the MAPK cascade is involved in the production of various pro-inflammatory cytokines, leading to various skin pathogenesis [38]. It is reported that AP-1, similar to NF-κB, contains transcriptional regulatory binding sites for most inflammatory mediators. AP-1 is also independent of the NF-κB binding promoter during inflammation [30].

Moreover, enhanced AP-1 transcription upregulates the expression of MMP genes (such as MMP-1 and MMP-3), which accelerates the degradation of the intercellular matrix (ECM), and further weakens the skin barrier function [31]. We explored the effects of UVB irradiation and LP-PBS on the mRNA expression levels of cytokines in the MAPK/AP-1 pathway in HaCaT using qRT-PCR. As shown in Figure 5a, UVB irradiation does indeed upregulate the expression levels of key cytokines in the MAPK/AP-1 pathway, thereby promoting the transmission of the MAPK/AP-1 pathway, and the downstream transcription of inflammatory factors and MMP genes, while LP-EPS treatment significantly protects HaCaT. As shown in Figure 6, the above results indicate that LP-EPS can effectively treat or ameliorate skin inflammation caused by UVB, which may be regulated by the NF-κB and MAPK/AP-1 pathways. Thus, our study proves that LP-EPS has excellent anti-inflammatory properties, and shows the potential application value of LP-EPS in skin care.
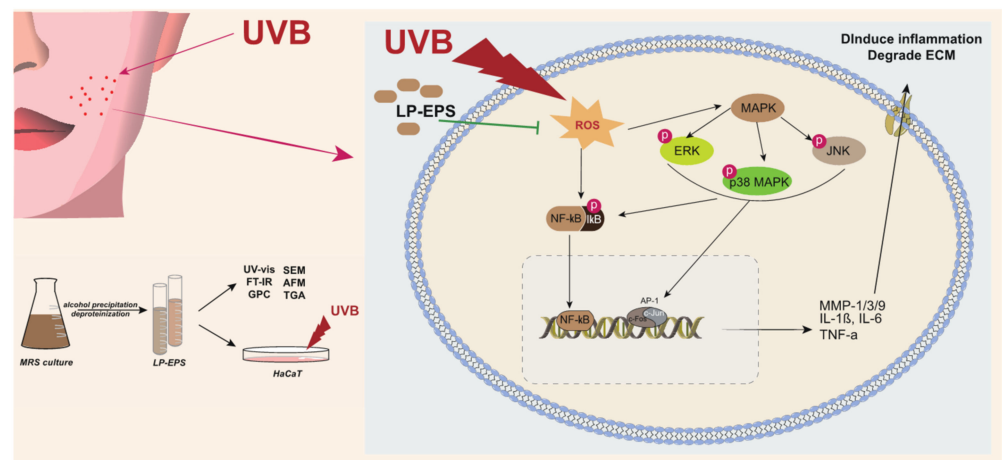


**Figure 6.** Pathways of action of LP-EPS to treat or ameliorate UVB-induced skin inflammation.

## 5. Conclusions

In this study, we isolated and purified the exopolysaccharides of *L. paracasei* subsp. *paracasei* SS-01 strain, characterized their structures, and analyzed their molecular properties. The functional groups of LP-EPS were identified using infrared spectroscopy, and SEM and AFM micrographs show that LP-EPS is a polysaccharide with a long-chain branching and multi-strand entangling structure, and a smooth rod-like or cloud-like state. Research on the biochemical, cellular, and biomolecular levels of LP-EPS show that it has great potential as an anti-inflammatory component, by virtue of being able to effectively remove intracellular ROS, and reduce the secretion of inflammation-related factors.

## References

1. Costa, O.Y.A.; De Hollander, M.; Pijl, A.; Liu, B.; Kuramae, E.E. Cultivation-independent and cultivation-dependent metagenomes reveal genetic and enzymatic potential of microbial community involved in the degradation of a complex microbial polymer. *Microbiome* **2020**, *8*, 76. [CrossRef] [PubMed]
2. Živković, M.; Miljković, M.S.; Ruas-Madiedo, P.; Markelić, M.B.; Veljović, K.; Tolinački, M.; Soković, S.; Korać, A.; Golić, N. EPS-SJ Exopolisaccharide Produced by the Strain *Lactobacillus paracasei* subsp. paracasei BGSJ2-8 Is Involved in Adhesion to Epithelial Intestinal Cells and Decrease on E. coli Association to Caco-2 Cells. *Front. Microbiol.* **2016**, *7*, 286. [CrossRef] [PubMed]
3. Chaisuwan, W.; Jantanasakulwong, K.; Wangtueai, S.; Phimolsiripol, Y.; Chaiyaso, T.; Techapun, C.; Phongthai, S.; You, S.G.; Regenstein, J.M.; Seesuriyachan, P. Microbial exopolysaccharides for immune enhancement: Fermentation, modifications and bioactivities. *Food Biosci.* **2020**, *35*, 100564. [CrossRef]
4. Lu, Y.; Han, S.; Zhang, S.; Wang, K.; Lv, L.; McClements, D.J.; Xiao, H.; Berglund, B.; Yao, M.; Li, L. The role of probiotic exopolysaccharides in adhesion to mucin in different gastrointestinal conditions. *Curr. Res. Food Sci.* **2022**, *5*, 581–589. [CrossRef] [PubMed]
5. Sun, Q.; Liu, P.; You, S.; Zhao, D.; Wang, C.; Zhang, J.; Wang, D.; Li, M. Protective effects of LPL-EPS-02 on human dermal fibroblasts damaged by UVA radiation. *J. Funct. Foods* **2021**, *83*, 104544. [CrossRef]
6. Jurášková, D.; Ribeiro, S.C.; Silva, C.C.G. Exopolysaccharides Produced by Lactic Acid Bacteria: From Biosynthesis to Health-Promoting Properties. *Foods* **2022**, *11*, 156. [CrossRef]
7. Monsan, P.; Bozonnet, S.; Albenne, C.; Joucla, G.; Willemot, R.M.; Remaud-Siméon, M. Homopolysaccharides from lactic acid bacteria. *Int. Dairy J.* **2001**, *11*, 675–685. [CrossRef]
8. Adebayo-Tayo, B.; Fashogbon, R. In vitro antioxidant, antibacterial, in vivo immunomodulatory, antitumor and hematological potential of exopolysaccharide produced by wild type and mutant *Lactobacillus delbureckii* subsp. bulgaricus. *Heliyon* **2020**, *6*, e03268. [CrossRef]
9. You, X.; Li, Z.; Ma, K.; Zhang, C.; Chen, X.; Wang, G.; Yang, L.; Dong, M.; Rui, X.; Zhang, Q.; et al. Structural characterization and immunomodulatory activity of an exopolysaccharide produced by *Lactobacillus helveticus* LZ-R-5. *Carbohydr. Polym.* **2020**, *235*, 115977. [CrossRef]
10. Angelin, J.; Kavitha, M. Exopolysaccharides from probiotic bacteria and their health potential. *Int. J. Biol. Macromol.* **2020**, *162*, 853–865. [CrossRef]
11. Shukla, A.; Gaur, P.; Aggarwal, A. Effect of probiotics on clinical and immune parameters in enthesitis-related arthritis category of juvenile idiopathic arthritis. *Clin. Exp. Immunol.* **2016**, *185*, 301. [CrossRef] [PubMed]
12. Kang, H.; Choi, H.S.; Kim, J.E.; Han, N.S. Exopolysaccharide-overproducing Lactobacillus paracasei KB28 induces cytokines in mouse peritoneal macrophages via modulation of NF-κβ and MAPKs. *J. Microbiol. Biotechnol.* **2011**, *21*, 1174–1178. [CrossRef] [PubMed]
13. Noda, M.; Danshiitsoodol, N.; Kanno, K.; Uchida, T.; Sugiyama, M. The Exopolysaccharide Produced by *Lactobacillus paracasei* IJH-SONE68 Prevents and Ameliorates Inflammatory Responses in DSS-Induced Ulcerative Colitis. *Microorganisms* **2021**, *9*, 2243. [CrossRef]
14. Noda, M.; Sultana, N.; Hayashi, I.; Fukamachi, M.; Sugiyama, M. Exopolysaccharide Produced by *Lactobacillus paracasei* IJH-SONE68 Prevents and Improves the Picryl Chloride-Induced Contact Dermatitis. *Molecules* **2019**, *24*, 2970. [CrossRef] [PubMed]
15. Robijn, G.W.; Wienk, H.L.J.; van den Berg, D.J.C.; Haas, H.; Kamerling, J.P.; Vliegenthart, J.F.G. Structural studies of the exopolysaccharide produced by *Lactobacillus paracasei* 34-1. *Carbohydr. Res.* **1996**, *285*, 129–139. [CrossRef]
16. Balzaretti, S.; Taverniti, V.; Guglielmetti, S.; Fiore, W.; Minuzzo, M.; Ngo, H.N.; Ngere, J.B.; Sadiq, S.; Humphreys, P.N.; Laws, A.P. A Novel Rhamnose-Rich Hetero-exopolysaccharide Isolated from *Lactobacillus paracasei* DG Activates THP-1 Human Monocytic Cells. *Appl. Environ. Microbiol.* **2017**, *83*, e02702-16. [CrossRef]
17. Li, L.; Huang, T.; Liu, H.; Zang, J.; Wang, P.; Jiang, X. Purification, structural characterization and anti-UVB irradiation activity of an extracellular polysaccharide from *Pantoea agglomerans*. *Int. J. Biol. Macromol.* **2019**, *137*, 1002–1012. [CrossRef]
18. Zhang, Y.; You, S.; Wang, D.; Zhao, D.; Zhang, J.; An, Q.; Li, M.; Wang, C. Fermented *Dendrobium officinale* polysaccharides protect UVA-induced photoaging of human skin fibroblasts. *Food Sci. Nutr.* **2022**, *10*, 1275–1288. [CrossRef]
19. Riaz Rajoka, M.S.; Mehwish, H.M.; Fang, H.; Padhiar, A.A.; Zeng, X.; Khurshid, M.; He, Z.; Zhao, L. Characterization and anti-tumor activity of exopolysaccharide produced by *Lactobacillus kefiri* isolated from Chinese kefir grains. *J. Funct. Foods* **2019**, *63*, 103588. [CrossRef]
20. Liu, Z.; Jiao, Y.; Lu, H.; Shu, X.; Chen, Q. Chemical characterization, antioxidant properties and anticancer activity of exopolysaccharides from *Floccularia luteovirens*. *Carbohydr. Polym.* **2020**, *229*, 115432. [CrossRef]
21. Min, W.H.; Fang, X.B.; Wu, T.; Fang, L.; Liu, C.L.; Wang, J. Characterization and antioxidant activity of an acidic exopolysaccharide from *Lactobacillus plantarum* JLAU103. *J. Biosci. Bioeng.* **2019**, *127*, 758–766. [CrossRef] [PubMed]
22. Wenping, L.; Hui, Z.; Qi, C.; Xingrong, Z.; Kun, W.; Jiaqi, W.C.L. Screening and Identification of Probiotics with Hyaluronidase Inhibitory Activity in Vitro. *Food Sci.* **2021**, *42*, 151–157. [CrossRef]
23. Zhang, Y.; Wang, D.; Fu, H.; Zhao, D.; Zhang, J.; Li, M.; Wang, C. Protective effects of extracellular proteins of Saccharomycopsis fibuligera on UVA-damaged human skin fibroblasts. *J. Funct. Foods* **2022**, *88*, 104897. [CrossRef]

24. Song, Q.; Jiang, L.; Yang, X.; Huang, L.; Yu, Y.; Yu, Q.; Chen, Y.; Xie, J. Physicochemical and functional properties of a water-soluble polysaccharide extracted from Mung bean (*Vigna radiate* L.) and its antioxidant activity. *Int. J. Biol. Macromol.* **2019**, *138*, 874–880. [CrossRef] [PubMed]

25. Xu, Y.; Cui, Y.; Wang, X.; Yue, F.; Shan, Y.; Liu, B.; Zhou, Y.; Yi, Y.; Lü, X. Purification, characterization and bioactivity of exopolysaccharides produced by *Lactobacillus plantarum* KX041. *Int. J. Biol. Macromol.* **2019**, *128*, 480–492. [CrossRef] [PubMed]

26. Zhao, D.; Jiang, J.; Du, R.; Guo, S.; Ping, W.; Ling, H.; Ge, J. Purification and characterization of an exopolysaccharide from *Leuconostoc lactis* L2. *Int. J. Biol. Macromol.* **2019**, *139*, 1224–1231. [CrossRef] [PubMed]

27. Asgher, M.; Urooj, Y.; Qamar, S.A.; Khalid, N. Improved exopolysaccharide production from *Bacillus licheniformis* MS3: Optimization and structural/functional characterization. *Int. J. Biol. Macromol.* **2020**, *151*, 984–992. [CrossRef]

28. Li, S.; Wu, Z.; Zhang, H.; Chen, W.G.B. Observation of Exopolysaccharide S2 from *Lactobacillus rhamnosus* KF5 Using Atomic Force Microscopy. *Food Sci.* **2015**, *36*, 43–47. [CrossRef]

29. Yang, Y.; Gong, W.; Jin, C.; Chen, Z.; Zhang, L.; Zou, Y.; Quan, S.; Huang, H. Naringin ameliorates experimental diabetic renal fibrosis by inhibiting the ERK1/2 and JNK MAPK signaling pathways. *J. Funct. Foods* **2018**, *50*, 53–62. [CrossRef]

30. Palomer, X.; Román-Azcona, M.S.; Pizarro-Delgado, J.; Planavila, A.; Villarroya, F.; Valenzuela-Alcaraz, B.; Crispi, F.; Sepúlveda-Martínez, Á.; Miguel-Escalada, I.; Ferrer, J.; et al. SIRT3-mediated inhibition of FOS through histone H3 deacetylation prevents cardiac fibrosis and inflammation. *Signal Transduct. Target. Ther.* **2020**, *5*, 14. [CrossRef]

31. Lee, Y.H.; Seo, E.K.; Lee, S.T. Skullcapflavone II inhibits degradation of type I collagen by suppressing MMP-1 transcription in human skin fibroblasts. *Int. J. Mol. Sci.* **2019**, *20*, 2734. [CrossRef]

32. Ansary, T.M.; Hossain, M.R.; Kamiya, K.; Komine, M.; Ohtsuki, M. Inflammatory molecules associated with ultraviolet radiation-mediated skin aging. *Int. J. Mol. Sci.* **2021**, *22*, 3974. [CrossRef] [PubMed]

33. Yujun, L.; Yuqing, Z.; Yuan, G.; Huanyu, L.; Guangqing Mou, Y. tuo Study on Antioxidant Activity of *Lactobacillus exopolysaccharides*. *J. Chinese Inst. Food Sci. Technol.* **2019**, *19*, 21–35. [CrossRef]

34. Noda, M.; Kanno, K.; Danshiitsoodol, N.; Higashikawa, F.; Sugiyama, M. Plant-derived lactobacillus paracasei ijh-sone68 improves chronic allergy status: A randomized, double-blind, placebo-controlled clinical trial. *Nutrients* **2021**, *13*, 4022. [CrossRef]

35. Noda, M.; Sugimoto, S.; Hayashi, I.; Danshiitsoodol, N.; Fukamachi, M.; Sugiyama, M. A novel structure of exopolysaccharide produced by a plant-derived lactic acid bacterium *Lactobacillus paracasei* IJH-SONE68. *J. Biochem.* **2018**, *164*, 87–92. [CrossRef]

36. Choi, S.I.; Jung, T.D.; Cho, B.Y.; Choi, S.H.; Sim, W.S.; Han, X.; Lee, S.J.; Kim, Y.C.; Lee, O.H. Anti-photoaging effect of fermented agricultural by-products on ultraviolet B-irradiated hairless mouse skin. *Int. J. Mol. Med.* **2019**, *44*, 559. [CrossRef]

37. Zhang, Y.; Fu, H.; Zhang, Y.; Wang, D.; Zhao, D.; Li, M.; Wang, C. Reparative Effects of Dandelion Fermentation Broth on UVB-Induced Skin Inflammation. *Clin. Cosmet. Investig. Dermatol.* **2022**, *15*, 471–482. [CrossRef]

38. Zhang, D.; Li, L.; Jiang, H.; Knolhoff, B.L.; Lockhart, A.C.; Wang-Gillam, A.; DeNardo, D.G.; Ruzinova, M.B.; Lim, K.H. Constitutive IRAK4 Activation Underlies Poor Prognosis and Chemoresistance In Pancreatic Ductal Adenocarcinoma. *Clin. Cancer Res.* **2017**, *23*, 1748. [CrossRef]